Chapter 8
Folding and Catalysis Near Life's Origin: Support for Fe^{2+} as a Dominant Divalent Cation

C. Denise Okafor, Jessica C. Bowman, Nicholas V. Hud, Jennifer B. Glass, and Loren Dean Williams

Abstract There is broad consensus that during and immediately following the origin of life, RNA was the single biopolymer or was among a small group of cooperating biopolymers. During the origin of life, the Archean Earth was anoxic; Fe^{2+} was abundant and relatively benign. We hypothesize that RNA used Fe^{2+} as a cofactor instead of, or along with, Mg^{2+} during the inception and early phases of biology, until the Great Oxidation Event (GOE). In this model, RNA participated in a metal substitution during the GOE, whereby Mg^{2+} replaced Fe^{2+} as the dominant RNA cofactor. A GOE-induced Fe^{2+} to Mg^{2+} substitution predicts that under 'early Earth' (anoxic) conditions, Fe^{2+} can participate in a variety of functions, including mediation of RNA folding and catalysis by ribozymes and proteins. Understanding the influence of Fe^{2+} on nucleic acid structure and function could provide an important link between the geological record and the ancestral biological world. This review focuses on experimental work investigating the interactions and functions of RNA and nucleic acid processing proteins with Fe^{2+} under anoxic, early Earth conditions.

8.1 Introduction

Cations play complex and essential roles in the folding of RNA into compact native states, in which negatively charged phosphate groups of the backbone are forced into close proximity (Brion and Westhof 1997; Hsiao et al. 2008). In association with folded RNAs, cations occupy a continuum of states distinguished by extent of direct

C. D. Okafor · J. C. Bowman · N. V. Hud · L. D. Williams (✉)
School of Chemistry and Biochemistry, NSF-NASA Center for Chemical Evolution, Georgia Institute of Technology, Atlanta, GA, USA
e-mail: loren.williams@chemistry.gatech.edu

J. B. Glass
School of Earth and Atmospheric Sciences, Georgia Institute of Technology, Atlanta, GA, USA

C. Menor-Salván (ed.), *Prebiotic Chemistry and Chemical Evolution of Nucleic Acids*, Nucleic Acids and Molecular Biology 35,
https://doi.org/10.1007/978-3-319-93584-3_8

coordination by RNA, thermodynamic contributions to folding, rates and dimensionalities of diffusion, and influence on specific structural states and on populations (Bowman et al. 2012). We partition this continuum of states into four classes: free, condensed, glassy, and chelated cations.

Condensed divalent cations are electrostatically linked to RNA and are found within envelopes that extend well beyond the van der Waals surface of the collapsed RNA. Condensed cations are fully hydrated, with near bulk-like diffusion properties. Glassy cations, with mobility restricted to one or two dimensions, are closely associated with RNA and are often partially dehydrated. Chelated cations, with two to four first-shell RNA ligands, can stabilize specific conformational states of the RNA. Chelated cations are less frequent than glassy ions, which are less frequent than condensed ions.

Cations assist with RNA catalysis by stabilizing transition states (Butcher 2011; Johnson-Buck et al. 2011) and/or by participating in catalysis (Hanna and Doudna 2000). Mg^{2+} is considered the dominant cofactor in ribozyme catalysis and in nucleic acid processing enzymes, and is one of the most abundant divalent cations in vivo (Draper 2004).

We have developed a model in which Fe^{2+}, in association with RNA and with nucleic acid processing enzymes, was a dominant divalent metal ion in life on the early Earth. We further postulate that Fe^{2+} complexes have been retained in certain extant anaerobes. Our recent results support a model in which iron, possibly along with magnesium, was a critical cofactor for nucleic acids during the Archean Eon. The anoxic and iron-rich (in combination, "ferruginous") conditions of the Archean would have inhibited destructive iron-mediated processes such as Fenton chemistry (Prousek 2007; Kozlowski et al. 2014), allowing Fe^{2+} to become deeply embedded in biological chemistry (Theil and Goss 2009).

Iron was abundant, soluble, and benign when life originated and first proliferated (Anbar 2008; Hazen and Ferry 2010; Holland 2006; Johnson et al. 2008). For around two billion years, the anoxic conditions of the ancient Earth sustained soluble Fe^{2+} rather than insoluble Fe^{3+} that is present in seawater today at picomolar concentrations. The abundance of iron in Archean seawater is evident from the extraordinary banded iron formations that span two billion years of the geologic rock record (Reinhard et al. 2017). It was originally assumed that in Archean seawater Fe^{2+} would be buffered at ~0.1 mM by equilibrium with ferrous carbonate (siderite, $FeCO_3$) (Holland 1973, 1984; Drever 1974). However, subsequent work has shown that siderite could have been strongly supersaturated in ancient oceans due to the slow kinetics of siderite precipitation. Instead, Derry (2015) suggests that ancient Fe^{2+} concentrations would have been controlled by the solubility of ferrous phosphate (vivianite), $3Fe^{2+} + 2HPO_4^{2-} + 8H_2O = Fe_3(PO_4)_2 \cdot 8H_2O + 2H^+$. The most recent estimates of Archean HPO_4^{2-} is 0.04–0.13 μM (Jones et al. 2015), which would yield $Fe^{2+} > 1$ mM (Derry 2015). Much less is known about seawater Mg^{2+} in the Archean, except that concentrations would have been lower than in modern oceans (~10 mM vs 52 mM Mg^{2+} in modern oceans) due to enhanced hydrothermal activity, which strips Mg^{2+} from seawater during hot-water-rock interactions in the ocean crust (Izawa et al. 2010). It is important to note that there

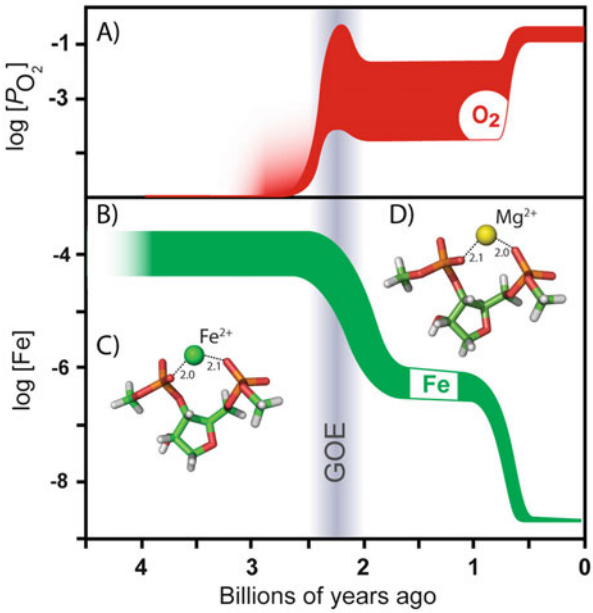

Fig. 8.1 Fe^{2+} was abundant in the biosphere before the Great Oxidation Event (GOE), when O_2 began to accumulate in the atmosphere. Approximate amount of (**a**) atmospheric O_2 and (**b**) dissolved iron in Earth's oceans over time. RNA coordinating (**c**) Fe^{2+} or (**d**) Mg^{2+}. Adapted from Lyons et al. (2014) and Anbar (2008). Vertical thickness of lines indicating O_2 and Fe^{2+} concentrations represent uncertainty in historical levels

are order-of-magnitude uncertainties for the ion content of Archean seawater (Holland et al. 2003), but the latest estimates suggest that Fe^{2+} and Mg^{2+} could have approached equimolar concentrations in the low mM in Archean seawater, while in modern oxic waters, Mg^{2+} is ~10 orders of magnitude more abundant than Fe^{2+}.

The Great Oxidation Event (GOE) forced the modern condition of iron scarcity and iron-mediated oxidative damage (Aguirre and Culotta 2012; Ushizaka et al. 2011; Martin and Imlay 2011; Cotruvo and Stubbe 2011; Wolfe-Simon et al. 2006; Anjem et al. 2009; Harel et al. 2014; Torrents et al. 2002). With the rise in oxygen, much of the Fe^{2+} of the early Earth was oxidized and geologically sequestered (Fig. 8.1). However, toxicity and vanishingly low concentrations of Fe^{2+} on the surface of the modern oxic Earth have not reversed the effects of iron's extensive evolutionary history and great utility in catalysis. Iron is the most abundant transition metal by far in human cells (Iyengar and Woittiez 1988).

The idea that Fe^{2+} played a crucial role in association with RNA on the early Earth is motivated by the theories that life may have originated (1) with RNA-based genetic and metabolic systems, i.e., the RNA world (Atkins et al. 2011), or (2) in a system of RNA-protein mutualism (Lanier et al. 2017). In both of these scenarios, and in essentially all models of the origin of life, RNA was an important component of early life in an anoxic, iron-rich environment. Therefore, understanding the influence of Fe^{2+} on nucleic acid structure and function could provide important links between the geological record and the ancestral biological world. This review focuses on work that has investigated the interactions of RNA, Fe^{2+}, and proteins under anoxic, early Earth conditions.

8.2 $Fe^{2+} \rightarrow Mg^{2+}$ Substitution

We hypothesize that RNA used Fe^{2+} as a cofactor when iron was benign and abundant, and experienced metal substitution during the GOE, whereby Mg^{2+} replaced Fe^{2+}. Among available cations in extant biology, Mg^{2+} is thought to have a special relationship with RNA (Bowman et al. 2012; Zheng et al. 2015). Mg^{2+} was seen early on to be especially important in folding of tRNA (Cole et al. 1972) and is now thought to be critical for folding of essentially all compact RNAs (Pyle 1993; Cate et al. 1996; Misra and Draper 1998). Mg^{2+} ions neutralize the negative charge of the RNA backbone and bind specifically to complex structural features of RNA (Petrov et al. 2012). Mg^{2+} is specifically required for activity of many ribozymes (Butcher 2011; Johnson-Buck et al. 2011) and essentially all nucleic acid processing enzymes. The small size, high charge density, and fixed oxidation state of Mg^{2+} compared with other biological cations makes it uniquely suited as a partner for RNA (Rashin and Honig 1985; Maguire and Cowan 2002; Brown 1992; Bock et al. 2006; Petrov et al. 2011). Mg^{2+} packs water molecules and RNA ligands tightly into its first coordination shell, orienting and polarizing water for molecular recognition and catalysis (Fig. 8.2a). Mg^{2+} and Fe^{2+} are characterized by similar coordination chemistry, supporting the plausibility of the $Fe^{2+} \rightarrow Mg^{2+}$ model (Table 8.1). The parameters of Table 8.1 suggest that Fe^{2+} and Mg^{2+} are similar in each of the classes of RNA association: free, condensed, glassy, and chelated. Our substitution hypothesis is based in part on analogy with metal substitution in some metalloproteins. The GOE resulted in decreases in Fe^{2+} concentrations and subsequent replacement in metabolic processes by other metals such as Cu^{2+}, Zn^{2+}, and Mn^{2+} (Aguirre and Culotta 2012; Ushizaka et al. 2011; Martin and Imlay 2011; Cotruvo and Stubbe 2011; Wolfe-Simon et al. 2006; Anjem et al. 2009; Harel et al. 2014; Torrents et al. 2002; Dupont et al. 2006, 2010).

Mg^{2+} coordinates RNA phosphate oxyanions with octahedral coordination geometry, bringing the first-shell ligands within ~2.1 angstroms of the metal ion. Quantum mechanics calculations show that the octahedral geometry of RNA-metal complexes and RNA conformation are conserved for Mg^{2+} or Fe^{2+} (Fig. 8.2) (Athavale et al. 2012).

A GOE-induced Fe^{2+} to Mg^{2+} substitution implies that under "early Earth" (anoxic) conditions, Fe^{2+} would have been able to perform a variety of functions, mediating RNA folding and acting as a cofactor for ribozyme and nucleic acid processing enzymes. In addition, because it is not limited to a single oxidation state, iron has the potential to confer redox functionality on RNA. In anoxia, Fe^{2+} would be unable to cleave RNA via the Fenton reaction (Prousek 2007; Kozlowski et al. 2014). For RNAs that are dependent on Mg^{2+} for folding or catalytic activity, structure and function should be conserved upon substitution of Mg^{2+} for Fe^{2+}. Likewise, nucleic acid processing proteins dependent on Mg^{2+} as a cofactor should be able to catalyze reactions with Fe^{2+}.

The $Fe^{2+} \rightarrow Mg^{2+}$ substitution hypothesis has been tested in vitro by reversing the putative substitution in anoxic conditions (Athavale et al. 2012; Okafor et al. 2017; Hsiao et al. 2013; Popovic et al. 2015). Mg^{2+} was removed and Fe^{2+} added to RNA

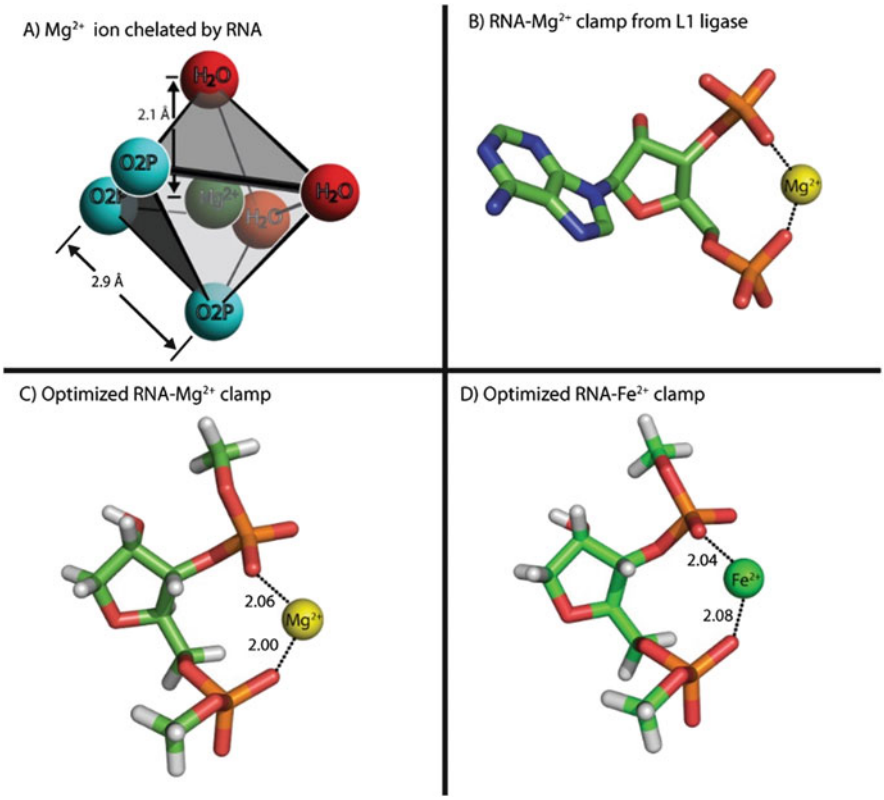

Fig. 8.2 (**a**) Mg^{2+} ion chelated by RNA. This Mg^{2+} ion (green sphere) is octahedral, with three first-shell phosphate oxygens of the rRNA (cyan) and three first-shell water oxygens (red). Mg^{2+}-oxygen distances are around 2.1 Å. (**b**) A first-shell RNA-Mg^{2+} complex: an RNA-Mg^{2+} clamp from the L1 ribozyme ligase (PDB 2OIU). (**c**) An RNA-Mg^{2+} clamp optimized by high-level QM calculations. (**d**) An optimized RNA-Fe^{2+} clamp. Each cation (Mg^{2+} or Fe^{2+}) is hexacoordinate. Mg^{2+} is shown as a yellow sphere, and Fe^{2+} is shown as a green sphere. Water molecules are omitted. Panel **a** adapted from Bowman et al. (2012). Panels **b**, **c**, and **d** from Athavale et al. (2012)

Table 8.1 Characteristics of Mg^{2+} and Fe^{2+}

	r (Å)[a]	AOCN[b]	$-\Delta H_{hyd}$[c]	pK_a[d]	ΔH[e]
Mg^{2+}	0.65	6	458[f]	11.4	
Fe^{2+}[g]	0.74	6	464[h]	9.5	−1.3

[a]Ionic radius (Brown 1988)
[b]Average observed coordination number (Brown 1988)
[c]Hydration enthalpy (kcal mol) (Brion and Westhof 1997)
[d]pK_a of $M^{2+}(H_2O)_6$ where $M^{2+} = Fe^{2+}$ or Mg^{2+} (Wulfsberg 1991)
[e]Interaction enthalpy relative to Mg^{2+} (kcal mol^{-1}) for RNA clamp formation (Dupont et al. 2010; Athavale et al. 2012). From Okafor et al. (2017)
[f]From Rashin and Honig (1985)
[g]High spin
[h]From Uudsemaa and Tamm (2004)

or to nucleic acid processing enzymes and their nucleic acid substrates. Structure probing experiments by Athavale et al. (2012) suggest that the conformation of P4–P6 domain RNA is conserved in the presence of Mg^{2+} or Fe^{2+}. Moreover, catalysis by the L1 ligase and hammerhead ribozymes is enhanced in the presence of Fe^{2+} compared to Mg^{2+} (Athavale et al. 2012). Popovic et al. (2015) demonstrated that, at neutral pH, Fe^{2+}-evolved ribozymes are more tolerant of Mg^{2+} substitution than Mg^{2+}-evolved ribozymes are of Fe^{2+} substitution. Hsiao et al. (2013) have shown that Fe^{2+} and some RNAs (P4–P6 domain, 23S rRNA, tRNA) catalyze single-electron transfer. Additionally, a DNA polymerase, RNA polymerase, and DNA ligase catalyze phosphodiester bond formation in the presence of Fe^{2+} and in the absence of Mg^{2+} (Okafor et al. 2017). The viability of an $Fe^{2+} \rightarrow Mg^{2+}$ substitution is also supported by consistencies in coordination chemistry (Athavale et al. 2012; Okafor et al. 2017).

8.3 Secondary Structure Probing of RNA Folding with Fe^{2+}

The secondary structure of the P4–P6 domain of *T. thermophila* group I intron was assayed by SHAPE (selective 2′-hydroxyl acylation analyzed by primer extension) in the presence of Na^{+}, Mg^{2+}, or Fe^{2+}. SHAPE is a powerful technique that provides secondary and tertiary structural information about RNAs at single-nucleotide resolution (Merino et al. 2005; Wilkinson et al. 2005). Briefly, local RNA flexibility is determined by the relative reactivities of ribose 2′-hydroxyl groups with an electrophile. The 2′-hydroxyl groups in RNA form adducts which, when reverse transcribed using fluorescently labeled primers, give truncated products. Resolution and visualization of fluorescent cDNA fragments using capillary electrophoresis permit the determination of RNA secondary structure based on the local flexibility of each nucleotide (Wilkinson et al. 2005, 2008).

In the presence of Na^{+}, the P4–P6 domain gave a SHAPE fingerprint consistent with the known secondary structure (Athavale et al. 2012; Cate et al. 1997). Upon addition of Mg^{2+}, SHAPE indicates that the structure of P4–P6 collapses to form long-range, tertiary interactions (Fig. 8.3). The structure obtained with Mg^{2+} is similar to previously reported SHAPE profiles for the same RNA in the presence of Mg^{2+} (Vicens et al. 2007).

The fingerprint of SHAPE reactivity for the P4–P6 domain RNA is conserved when Mg^{2+} is replaced by Fe^{2+} under anoxic conditions. This result suggests that tertiary interactions as well as specific and non-specific Mg^{2+}-RNA interactions are recapitulated by Fe^{2+} in the absence of oxygen. Fe^{2+} appears to be a true mimic for Mg^{2+} during RNA folding.

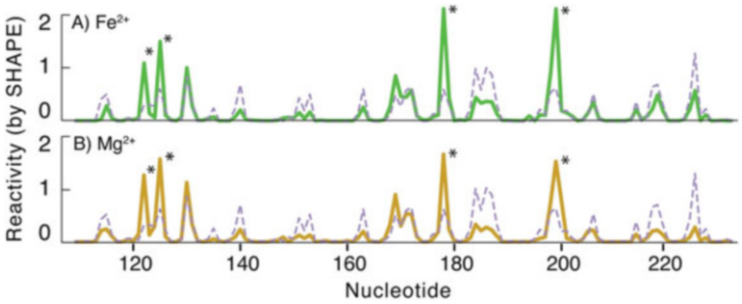

Fig. 8.3 Similar changes are observed in SHAPE reactivity with addition of Mg^{2+} or Fe^{2+}. (**a**) SHAPE profile of P4–P6 domain RNA in the presence of 250 mM NaCl and 2.5 mM Fe^{2+} (green) or 250 mM NaCl alone (purple, dashed). (**b**) SHAPE profile in the presence of 250 mM NaCl and 2.5 mM Mg^{2+} (yellow) or 250 mM NaCl alone (purple, dashed). Asterisks indicate sites with increased reactivity upon addition of divalent metal. Adapted from Athavale et al. (2012)

8.4 Ribozyme Activity with Fe^{2+}

We have also shown that Fe^{2+} is a good replacement for Mg^{2+} in mediating ribozyme catalysis (Athavale et al. 2012). The activity of two ribozymes was assayed in the presence of Mg^{2+} or Fe^{2+}. Both ribozymes displayed higher activity with Fe^{2+} than with Mg^{2+} (Table 8.2).

The L1 ribozyme ligase is an in vitro-selected, Mg^{2+}-dependent ribozyme that catalyzes formation of a phosphodiester linkage (Robertson and Scott 2007). Mg^{2+} coordinates non-bridging phosphate oxygens in the catalytic pocket, possibly stabilizing the negative charge developing in the transition state during catalysis.

The hammerhead ribozyme, which is widely distributed in the tree of life, cleaves the RNA backbone in a site-specific, reversible reaction, via nucleophilic attack by a 2′-hydroxyl group on the 3′-phosphorous atom (Scott 2007; Penedo et al. 2004). A cyclic 2′3′-phosphate is formed followed by departure of a phosphate oxygen as a 5′-hydroxyl. Divalent metal ions stabilize tertiary interactions and transition states in the ribozyme. Catalytic activity is observed in the folded ribozyme at low mM Mg^{2+} concentrations. While there is no evidence to show that divalent metals play a chemical role in catalysis, reduced activity is observed in the presence of monovalent ions only (Leclerc 2010). Divalent metal ions interacting with the hammerhead ribozyme likely remain hydrated.

The initial rate of ligation in L1 ligase was 25-fold higher in the presence of Fe^{2+} than Mg^{2+}, while the initial rate of hammerhead cleavage was 3.5-fold higher in the presence of Fe^{2+} than Mg^{2+} (Athavale et al. 2012). The observed enhancement in activities of these ribozymes indicates that Fe^{2+} substitutes for Mg^{2+} and facilitates catalysis not only in a case where the divalent metal directly participates in catalysis, as in the case of L1 ligase, but also in a case where Mg^{2+} may play non-specific supportive roles.

Popovic et al. (2015) used in vitro evolution to explore RNA function under early Earth conditions and to compare ribozyme populations that emerge under iron-rich

Table 8.2 Initial rates of ribozyme activity

	L1 ligase in 100 μM divalent	Hammerhead ribozyme in 25 μM divalent
Mg^{2+}	1.4×10^{-6} min^{-1}	1.1×10^{-2} min^{-1}
Fe^{2+}	3.5×10^{-5} min^{-1}	3.5×10^{-2} min^{-1}
k_{Fe}/k_{Mg}	25	3.5

From Athavale et al. (2012)

conditions with those obtained in the presence of Mg^{2+}. Self-cleaving ribozymes from the same starting library were evolved with Mg^{2+} or Fe^{2+} at pH 5 or pH 7 through four to seven selection steps and then evolved once more with the same or opposite ion. Evolved populations were compared, and the impact of metal ion identity and pH on ribozyme sequence examined. Both ion identity and pH were shown to favor evolution of specific ribozyme motifs. At pH 7, the dominant products of the selection were the same for both ions. However, the prevalence of hammerhead family motifs was greater in Fe^{2+} compared to Mg^{2+}. This result is consistent with prior work by Athavale et al. (2012) (Table 8.2) demonstrating enhanced hammerhead ribozyme activity in the presence of Fe^{2+} at pH 7.5. Ribozyme populations evolved in Fe^{2+} at pH 7 showed relatively little sensitivity to the substitution of Fe^{2+} for Mg^{2+}, but dominant motif families evolved in Mg^{2+} were perturbed by the substitution of Fe^{2+}. This observation appears to be consistent with the substitution of Fe^{2+} with Mg^{2+} over time in biopolymers, as the availability of Fe^{2+} declined in concert with the rise in atmospheric O_2. Populations evolved in Mg^{2+} or Fe^{2+} at pH 5 diverged from each other and those evolved at pH 7, suggesting that pH could have been an important factor in the ability of Mg^{2+} to replace Fe^{2+} in RNA function (Popovic et al. 2015).

8.5 Fe^{2+}-Mediated RNA Oxidoreduction

Fe^{2+} is able to confer oxidoreductase ability to RNA (Hsiao et al. 2013). In the absence of Mg^{2+} and under early Earth conditions, certain RNAs are observed to gain the ability to catalyze electron transfer in the presence of Fe^{2+}. We used a peroxidase assay, wherein H_2O_2 oxidizes a reducing agent, tetramethylbenzidine (TMB), to form a radical cation $TMB^{\bullet+}$ that absorbs at 652 nm (Josephy et al. 1982), to show that RNA-Fe^{2+} is a functional analog of horseradish peroxidase in catalyzing oxidoreduction. Oxidoreductase activity was observed in certain RNAs like P4–P6, 23S rRNA, the a-rRNA model of the ancestral ribosome, yeast $tRNA^{Phe}$, and Domain III of the 23S rRNA (Fig. 8.4). The activity was not observed in other RNAs such as a short duplex, a large unstructured RNA (satellite tobacco mosaic virus RNA), and a small single-stranded RNA. Activity was not observed with DNA or single nucleotides (ATP). Activity was also not observed in the absence of RNA or with any metal other than Fe^{2+}. In fact, the addition of other metals to the assay (e.g., Mg^{2+}, Na^{+}) was shown to attenuate oxidoreduction (Hsiao et al. 2013).

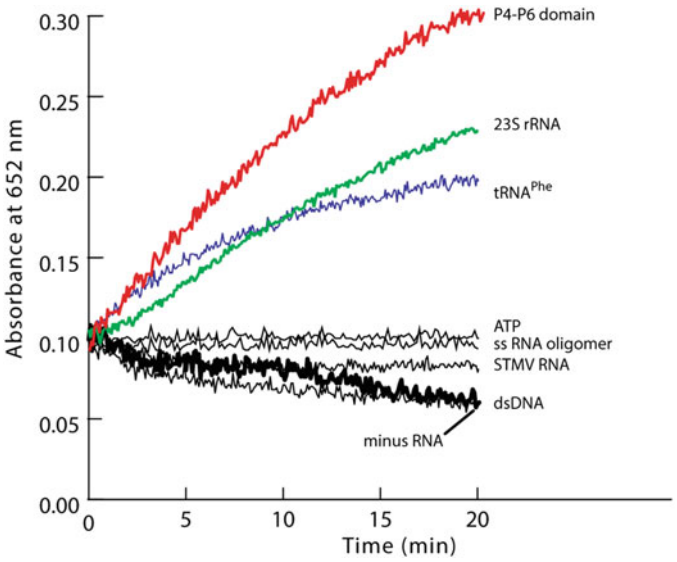

Fig. 8.4 Some RNAs (23S rRNA from *T. thermophilus*, P4–P6 domain RNA, yeast $tRNA^{Phe}$) in combination with Fe^{2+} catalyze single-electron transfer. Other nucleic acids (ATP, a short RNA oligomer, double-stranded DNA (dsDNA), and the RNA genome of STMV) are inefficient catalysts. All reactions were performed in the absence of O_2 and Mg^{2+} and in the presence of Fe^{2+}, tetramethylbenzidine, and H_2O_2. Adapted from Hsiao et al. (2013)

A Michaelis-Menten kinetic analysis of the oxidoreduction activity in RNA-Fe^{2+} complexes shows behavior consistent with true catalysis (Hsiao et al. 2013). Rate saturation was observed with increasing substrate concentration, and kinetic parameters were extracted from the data (Hsiao et al. 2013). While the RNA requirements for catalytic activity are not completely understood, the ability to coordinate Mg^{2+} ions is seen in all RNAs exhibiting catalysis, hinting at the importance of RNA coordination for Fe^{2+}-induced oxidoreductase activity.

It seems likely that chemical transformations such as oxidoreduction would have been required in primitive biological systems (Deamer and Weber 2010). RNA in combination with Fe^{2+} under pre-GOE conditions is indeed shown to catalyze oxidoreductase reactions, suggesting that the catalytic repertoire of RNA may have been much greater on an early Earth and was attenuated with the rise of O_2.

8.6 Fe^{2+} as a Mg^{2+} Substitute in Nucleic Acid Processing Enzymes

It is generally accepted that, in extant biology, nucleic acid processing enzymes such as ligases, polymerases, and kinases use a dual Mg^{2+} ion mechanism for catalysis (Fig. 8.5) (Rittié and Perbal 2008; Yang et al. 2006; Steitz 1999; Doherty and

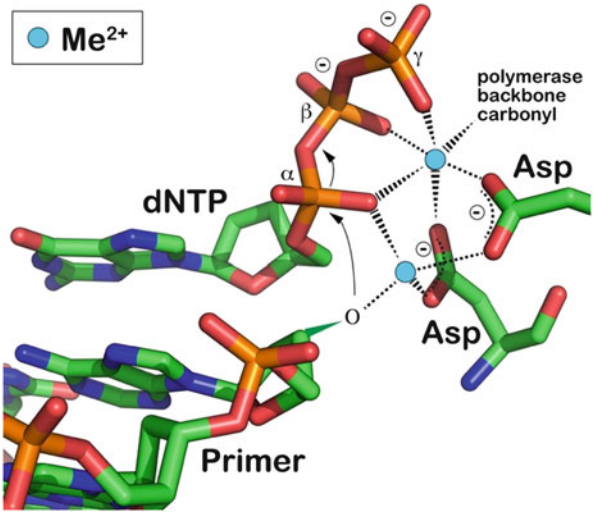

Fig. 8.5 Divalent cations are cofactors for protein enzymes that process nucleic acids. In a generally accepted mechanism for DNA and RNA polymerases (Steitz 1999; Lykke-Andersen and Christiansen 1998; Yin and Steitz 2004; Doublie et al. 1998), two divalent metal cations (Me^{2+}) stabilize the 5′ phosphate(s) of an incoming nucleotide and activate the 3′ hydroxyl of an existing nucleic acid polymer for nucleophilic attack, facilitating phosphodiester bond formation. Mechanism adapted from Steitz (1999), illustrated with PDB 1T7P (Doublie et al. 1998). This structure uses a dideoxy NTP and the position of the primer ribose 3′-OH is approximated. Waters are omitted for clarity

Dafforn 2000; Lee et al. 2000; Ellenberger and Tomkinson 2008; Lykke-Andersen and Christiansen 1998; Yin and Steitz 2004). We have begun to test the hypothesis that prior to the GOE, the dominant divalent cation was Fe^{2+} instead of Mg^{2+} in these protein-based nucleic processing enzymes (Okafor et al. 2017). Under anoxic conditions, Mg^{2+} was removed from three enzymes and replaced with Fe^{2+}. Thermostable Deep Vent (exo-) DNA polymerase, T7 RNA polymerase, and T4 DNA ligase all showed catalytic activity using Fe^{2+} instead of Mg^{2+} as a cofactor.

The ability of a DNA polymerase [Deep vent (exo-)] to amplify a DNA fragment in the presence of various divalent cations was tested by PCR. Product DNA was observed at the same PCR cycle number with Fe^{2+}, Mg^{2+}, or Mn^{2+} cofactors. The ability of T7 RNA polymerase to synthesize RNA was also assayed with Mg^{2+} or Fe^{2+}. A maximum yield was obtained with 0.75 mM Fe^{2+} compared to 6 mM Mg^{2+}, an eightfold difference. The ability of T4 DNA ligase to synthesize RNA was also assayed with Mg^{2+} or Fe^{2+}. The results show that Fe^{2+} can act as a cofactor for this DNA ligase.

In all enzymes investigated, control reactions were performed in the absence of divalent metals. No product was observed in controls, validating the methods used for Mg^{2+} extraction in the study, and confirming that enzyme activity in samples containing Fe^{2+} was due to enzyme utilization of added Fe^{2+} rather than residual Mg^{2+}.

8.7 Theoretical Support for Iron as an Ancient Cofactor of Catalysis

In both ribozymes and protein enzymes, Fe^{2+} appears to be a more potent cofactor than Mg^{2+}. Lower Fe^{2+} concentrations are required to achieve optimal catalysis in RNA polymerases, and increased activity was seen with Fe^{2+} over Mg^{2+} in both L1 ligase and hammerhead ribozymes (Athavale et al. 2012). Quantum mechanics calculations provide explanations for this observation [Table 8.1, (Athavale et al. 2012; Okafor et al. 2017)]. While conformations and geometries are highly similar between Fe^{2+} and Mg^{2+} complexes, differences were observed in metal interactions with water and phosphorus atom chemistry. When interaction energies were decomposed into charge transfer, polarization and exchange, divalent metal (M^{2+}) hexa-aquo complexes showed greater depletion of electrons from Fe^{2+}-coordinated water molecules than Mg^{2+}-coordinated waters. $Fe^{2+}(H_2O)_6$ is a stronger acid than $Mg^{2+}(H_2O)_6$, suggesting a greater frequency of occurrence of the $M^{2+}(H_2O)_5(OH^-)$ species of Fe^{2+} than Mg^{2+}. As most ribozyme mechanisms involve a nucleophilic attack by the deprotonated ribose 2′-OH group (Lilley 2011), the higher acidity of Fe^{2+} in the M^{2+} $(H_2O)_6$ complex may be more favorable for facilitating ribozyme catalysis than Mg^{2+}.

Additionally, the presence of lower lying d orbitals in Fe^{2+} have the effect of increased electron-withdrawing power compared to Mg^{2+}, making the phosphorus of phosphate a better electrophile with Fe^{2+} than with Mg^{2+}. Finally, Fe^{2+} displays increased affinity for oxygen atoms in the first coordination shell. Both of these properties affect rates of nucleophilic attack on phosphorus which modulates the observed rate of catalysis. However, the calculations do not explain why higher Fe^{2+} concentrations inhibit catalysis by a protein enzyme as observed by Okafor et al. (2017).

8.8 Iron-RNA in Extant Biology

Methods for mitigation of iron toxicity are widely distributed in biological systems. The iron-trafficking protein ferritin is ubiquitous in animal cells and found in most aerobic prokaryotes (Barton 2005). In animals, ferritin expression is controlled by iron regulatory proteins (IRPs) that bind the noncoding iron-responsive element (IRE) of ferritin mRNA during iron scarcity and repress translation (Ma et al. 2012). It has been suggested that the ferritin IRE is the ancestor of this type of translational control in more recent key metabolic proteins such as mitochondrial aconitase (mACO; Piccinelli and Samuelsson 2007). Fe^{2+} was shown to affect binding of iron regulatory protein 1 (IRP1) to ferritin and mACO IREs by inducing destabilizing conformational changes in the IREs, which result in decreased binding of IRP1 (Khan et al. 2009). Diminished binding of IRE RNA to IRP1 is also seen with Mg^{2+} but at 100 times the concentration of Fe^{2+} (Khan et al. 2009).

Failure of cellular iron regulatory systems has medical implications. Accumulation of redox-active iron correlates with the development and progression of

Alzheimer's disease (AD) (Smith et al. 2010). Oxidized cytoplasmic RNA is found in neurons vulnerable to AD (Nunomura et al. 1999). RNAs in AD brains are associated with Fe^{2+}; rRNA, and mRNA show twice as much iron binding as tRNA (Honda et al. 2005). Ribosomes purified from AD brains have reduced ability to perform translation, contain Fe^{2+}, and are redox active, potentially serving as "redox centers" for oxidation of cytoplasmic RNA (Honda et al. 2005).

8.9 Iron-RNA Research Methodology

The Fenton reaction, using Fe^{2+} to generate hydroxyl radical, was initially developed by Tullius and coworkers to probe nucleic acid structure (Tullius and Greenbaum 2005; Powers and Noller 1995; Tullius and Dombroski 1985; Berens et al. 1998; Celander and Cech 1990; Latham and Cech 1989; Burkhoff and Tullius 1987). Hydroxyl radical footprinting uses EDTA-chelated iron(II) to decompose H_2O_2, producing hydroxyl radicals, and $^{\bullet}OH$, which cleave nucleic acid backbones (Shcherbakova and Mitra 2009). Changes in the patterns of $^{\bullet}OH$ reactivity can be used to monitor groove width of DNA (Price and Tullius 1993) and compact structures of RNA (Latham and Cech 1989). Fe^{2+} was used to probe divalent binding sites in RNA, replacing Mg^{2+} at ion-binding sites and cleaving RNA in proximity of these sites via Fenton chemistry (Berens et al. 1998). This work showed that Mg^{2+} and Fe^{2+} compete for the same binding sites in the *Tetrahymena* group I intron (Berens et al. 1998). Fe^{2+}-EDTA tethered to a small molecule such as ethidium (Dervan 1986; Vary and Vournakis 1984; Kean et al. 1985) or to deoxyribonucleotides (Moser and Dervan 1987; Chu and Orgel 1985) has also been used to probe nucleic acids.

8.10 Summary

The conditions on early Earth (anoxic, high availability of soluble iron) were conducive for RNA-Fe^{2+} or RNA-Fe^{2+} protein biology and, as illustrated here, could have sustained an early Earth where Fe^{2+} was the primary cationic cofactor for RNA and proteins, later to be replaced by Mg^{2+} as free iron was sequestered.

There is strong evidence that Fe^{2+}, under anoxic conditions, can interact with RNA and proteins in a manner that closely resembles Mg^{2+}. However only a small, recent body of work aims to directly understand the structural and conformational features of RNA-Fe^{2+} complexes and the role of RNA-Fe^{2+}-protein interactions in nucleic acid processing. Fe^{2+} experimental studies are largely complicated by the high oxidation potential of Fe^{2+} to Fe^{3+} (-0.77 V). In the presence of oxygen, Fe^{2+} readily oxidizes to Fe^{3+} and/or promotes RNA degradation. Anoxic laboratory conditions are therefore crucial for experiments addressing the importance of Fe^{2+}.

In comparison with Mg^{2+}, Fe^{2+} is a more potent activator of RNA and at least some nucleic acid processing proteins. The minimum concentration for RNA folding is

lower for Fe^{2+} than for Mg^{2+}. At least some ribozymes are more active with Fe^{2+} than with Mg^{2+}. T7 RNA polymerase is far more active at low Fe^{2+} concentrations than in low Mg^{2+}. The minimum concentration for inline cleavage is lower for Fe^{2+} than for Mg^{2+} (Okafor, Hud, and Williams, unpublished). RNA-Fe^{2+} has more diverse chemical functionality, including catalysis of redox chemistry, than RNA-Mg^{2+}.

Recent Fe^{2+} experiments in simulated early Earth conditions have begun to examine the relevance of pH. More RNA-Fe^{2+} studies that vary other environmental factors, such as temperature and buffer components, under early Earth conditions, will be invaluable for increased understanding of Fe^{2+} interactions with RNA and protein pre-GOE.

Acknowledgments This work was supported in part by National Aeronautics and Space Administration grants NNX16AJ28G and NNX16AJ29G.

References

Aguirre JD, Culotta VC (2012) Battles with iron: manganese in oxidative stress protection. J Biol Chem 287:13541–13548

Anbar AD (2008) Oceans. Elements and evolution. Science 322:1481–1483

Anjem A, Varghese S, Imlay JA (2009) Manganese import is a key element of the oxyr response to hydrogen peroxide in *Escherichia coli*. Mol Microbiol 72:844–858

Athavale SS, Petrov AS, Hsiao C, Watkins D, Prickett CD, Gossett JJ, Lie L, Bowman JC, O'Neill E, Bernier CR et al (2012) RNA folding and catalysis mediated by iron (II). PLoS One 7:e38024

Atkins JF, Gesteland RF, Cech TR (eds) (2011) RNA worlds: from life's origins to diversity in gene regulation. Cold Spring Harbor Laboratory Press, Cold Spring Harbor, NY

Barton L (2005) Structural and functional relationships in prokaryotes. Springer, Berlin

Berens C, Streicher B, Schroeder R, Hillen W (1998) Visualizing metal-ion-binding sites in group I introns by iron(II)-mediated fenton reactions. Chem Biol 5:163–175

Bock CW, Markham GD, Katz AK, Glusker JP (2006) The arrangement of first- and second-shell water molecules around metal ions: effects of charge and size. Theor Chem Accounts 115:100–112

Bowman JC, Lenz TK, Hud NV, Williams LD (2012) Cations in charge: magnesium ions in RNA folding and catalysis. Curr Opin Struct Biol 22:262–272

Brion P, Westhof E (1997) Hierarchy and dynamics of RNA folding. Annu Rev Biophys Biomol Struct 26:113–137

Brown ID (1988) What factors determine cation coordination numbers. Acta Crystallogr Sect B 44:545–553

Brown ID (1992) Chemical and steric constraints in inorganic solids. Acta Crystallogr Sect B 48:553–572

Burkhoff AM, Tullius TD (1987) The unusual conformation adopted by the adenine tracts in kinetoplast DNA. Cell 48:935–943

Butcher SE (2011) The spliceosome and its metal ions. Met Ions Life Sci 9:235–251

Cate JH, Gooding AR, Podell E, Zhou K, Golden BL, Kundrot CE, Cech TR, Doudna JA (1996) Crystal structure of a group I ribozyme domain: principles of RNA packing. Science 273:1678–1685

Cate JH, Hanna RL, Doudna JA (1997) A magnesium ion core at the heart of a ribozyme domain. Nat Struct Biol 4:553–558

Celander DW, Cech TR (1990) Iron (II)-ethylenediaminetetraacetic acid catalyzed cleavage of RNA and DNA oligonucleotides: similar reactivity toward single-and double-stranded forms. Biochemistry 29:1355–1361
Chu BC, Orgel LE (1985) Nonenzymatic sequence-specific cleavage of single-stranded DNA. Proc Natl Acad Sci USA 82:963–967
Cole PE, Yang SK, Crothers DM (1972) Conformational changes of transfer ribonucleic acid. Equilibrium phase diagrams. Biochemistry 11:4358–4368
Cotruvo JA, Stubbe J (2011) Class I ribonucleotide reductases: metallocofactor assembly and repair *in vitro* and *in vivo*. Annu Rev Biochem 80:733–767
Deamer D, Weber AL (2010) Bioenergetics and life's origins. Cold Spring Harb Perspect Biol 2: a004929
Derry LA (2015) Causes and consequences of mid-proterozoic anoxia. Geophys Res Lett 42:8538–8546
Dervan P (1986) Design of sequence-specific DNA binding molecules. Science 232:464–471
Doherty AJ, Dafforn TR (2000) Nick recognition by DNA ligases. J Mol Biol 296:43–56
Doublie S, Tabor S, Long AM, Richardson CC, Ellenberger T (1998) Crystal structure of a bacteriophage T7 DNA replication complex at 2.2 Å resolution. Nature 391:251–258
Draper DE (2004) A guide to ions and RNA structure. RNA 10:335–343
Drever JI (1974) Geochemical model for the origin of precambrian banded iron formations. GSA Bull 85:1099–1106
Dupont CL, Yang S, Palenik B, Bourne PE (2006) Modern proteomes contain putative imprints of ancient shifts in trace metal geochemistry. Proc Natl Acad Sci USA 103:17822–17827
Dupont CL, Butcher A, Valas RE, Bourne PE, Caetano-Anolles G (2010) History of biological metal utilization inferred through phylogenomic analysis of protein structures. Proc Natl Acad Sci USA 107:10567–10572
Ellenberger T, Tomkinson AE (2008) Eukaryotic DNA ligases: structural and functional insights. Annu Rev Biochem 77:313
Hanna R, Doudna JA (2000) Metal ions in ribozyme folding and catalysis. Curr Opin Chem Biol 4:166–170
Harel A, Bromberg Y, Falkowski PG, Bhattacharya D (2014) Evolutionary history of redox metal-binding domains across the tree of life. Proc Natl Acad Sci USA 111:7042–7047
Hazen RM, Ferry JM (2010) Mineral evolution: mineralogy in the fourth dimension. Elements 6:9–12
Holland HD (1973) The oceans; a possible source of iron in iron-formations. Econ Geol 68:1169–1172
Holland H (1984) The chemical evolution of the atmosphere and oceans. Princeton University Press, Princeton, NJ
Holland HD (2006) The oxygenation of the atmosphere and oceans. Philos Trans R Soc B Biol Sci 361:903–915
Holland DM, Jacobs SS, Jenkins A (2003) Modelling the ocean circulation beneath the ross ice shelf. Antarct Sci 15:13–23
Honda K, Smith MA, Zhu X, Baus D, Merrick WC, Tartakoff AM, Hattier T, Harris PL, Siedlak SL, Fujioka H et al (2005) Ribosomal RNA in Alzheimer disease is oxidized by bound redox-active iron. J Biol Chem 280:20978–20986
Hsiao C, Tannenbaum M, VanDeusen H, Hershkovitz E, Perng G, Tannenbaum A, Williams LD (2008) In: Hud N (ed) Nucleic acid metal ion interactions. The Royal Society of Chemistry, London, pp 1–35
Hsiao C, Chou I-C, Okafor CD, Bowman JC, O'Neill EB, Athavale SS, Petrov AS, Hud NV, Wartell RM, Harvey SC et al (2013) Iron(II) plus RNA can catalyze electron transfer. Nat Chem 5:525–528
Iyengar V, Woittiez J (1988) Trace elements in human clinical specimens: evaluation of literature data to identify reference values. Clin Chem 34:474–481
Izawa MRM, Nesbitt HW, MacRae ND, Hoffman EL (2010) Composition and evolution of the early oceans: evidence from the tagish lake meteorite. Earth Planet Sci Lett 298:443–449

Johnson CM, Beard BL, Roden EE (2008) The iron isotope fingerprints of redox and biogeochemical cycling in modern and ancient earth. Annu Rev Earth Planet Sci 36:457–493
Johnson-Buck AE, McDowell SE, Walter NG (2011) Metal ions: supporting actors in the playbook of small ribozymes. Met Ions Life Sci 9:175–196
Jones C, Nomosatryo S, Crowe SA, Bjerrum CJ, Canfield DE (2015) Iron oxides, divalent cations, silica, and the early earth phosphorus crisis. Geology 43:135–138
Josephy PD, Eling T, Mason RP (1982) The horseradish peroxidase-catalyzed oxidation of 3,5,3',5'-tetramethylbenzidine. Free radical and charge-transfer complex intermediates. J Biol Chem 257:3669–3675
Kean JM, White SA, Draper DE (1985) Detection of high-affinity intercalator sites in a ribosomal RNA fragment by the affinity cleavage intercalator methidiumpropyl-EDTA-Iron(II). Biochemistry 24:5062–5070
Khan MA, Walden WE, Goss DJ, Theil EC (2009) Direct Fe^{2+} sensing by iron-responsive messenger RNA: repressor complexes weakens binding. J Biol Chem 284:30122–30128
Kozlowski H, Kolkowska P, Watly J, Krzywoszynska K, Potocki S (2014) General aspects of metal toxicity. Curr Med Chem 21:3721–3740
Lanier KA, Petrov AS, Williams LD (2017) The central symbiosis of molecular biology. J Mol Evol 85:8–13
Latham JA, Cech TR (1989) Defining the inside and outside of a catalytic RNA molecule. Science 245:276–282
Leclerc F (2010) Hammerhead ribozymes: true metal or nucleobase catalysis? Where is the catalytic power from? Molecules 15:5389
Lee JY, Chang C, Song HK, Moon J, Yang JK, Kim H-K, Kwon S-T, Suh SW (2000) Crystal structure of Nad(+)-dependent DNA ligase: modular architecture and functional implications. EMBO J 19:1119–1129
Lilley DMJ (2011) Mechanisms of RNA catalysis. Philos Trans R Soc B Biol Sci 366:2910–2917
Lykke-Andersen J, Christiansen J (1998) The C-terminal carboxy group of T7 RNA polymerase ensures efficient magnesium ion-dependent catalysis. Nucleic Acids Res 26:5630–5635
Lyons TW, Reinhard CT, Planavsky NJ (2014) The rise of oxygen in earth's early ocean and atmosphere. Nature 506:307–315
Ma J, Haldar S, Khan MA, Sharma SD, Merrick WC, Theil EC, Goss DJ (2012) Fe^{2+} binds iron responsive element-RNA, selectively changing protein-binding affinities and regulating mRNA repression and activation. Proc Natl Acad Sci USA 109:8417–8422
Maguire ME, Cowan JA (2002) Magnesium chemistry and biochemistry [review]. BioMetals 15:203–210
Martin JE, Imlay JA (2011) The alternative aerobic ribonucleotide reductase of *Escherichia coli*, Nrdef, is a manganese-dependent enzyme that enables cell replication during periods of iron starvation. Mol Microbiol 80:319–334
Merino EJ, Wilkinson KA, Coughlan JL, Weeks KM (2005) RNA structure analysis at single nucleotide resolution by selective 2'-hydroxyl acylation and primer extension (shape). J Am Chem Soc 127:4223–4231
Misra VK, Draper DE (1998) On the role of magnesium ions in RNA stability. Biopolymers 48:113–135
Moser HE, Dervan PB (1987) Sequence-specific cleavage of double helical DNA by triple helix formation. Science 238:645–650
Nunomura A, Perry G, Pappolla MA, Wade R, Hirai K, Chiba S, Smith MA (1999) RNA oxidation is a prominent feature of vulnerable neurons in Alzheimer's disease. J Neurosci 19:1959–1964
Okafor CD, Lanier KA, Petrov AS, Athavale SS, Bowman JC, Hud NV, Williams LD (2017) Iron mediates catalysis of nucleic acid processing enzymes: support for Fe(II) as a cofactor before the great oxidation event. Nucleic Acids Res 45:3634–3642
Penedo JC, Wilson TJ, Jayasena SD, Khvorova A, Lilley DM (2004) Folding of the natural hammerhead ribozyme is enhanced by interaction of auxiliary elements. RNA 10:880–888

Petrov AS, Bowman JC, Harvey SC, Williams LD (2011) Bidentate RNA-magnesium clamps: on the origin of the special role of magnesium in RNA folding. RNA 17:291–297
Petrov A, Bernier C, Hsiao C, Okafor CD, Tannenbaum E, Stern J, Gaucher E, Schneider D, Hud NV, Harvey SC et al (2012) RNA-magnesium-protein interactions in large ribosomal subunit. J Phys Chem B 116:8113–8120
Piccinelli P, Samuelsson T (2007) Evolution of the iron-responsive element. RNA 13:952–966
Popovic M, Fliss PS, Ditzler MA (2015) In vitro evolution of distinct self-cleaving ribozymes in diverse environments. Nucleic Acids Res 43:3789–3801
Powers T, Noller H (1995) Hydroxyl radical footprinting of ribosomal proteins on 16S rRNA. RNA 1:194
Price MA, Tullius TD (1993) How the structure of an adenine tract depends on sequence context: a new model for the structure of T_na_n DNA sequences. Biochemistry 32:127–136
Prousek J (2007) Fenton chemistry in biology and medicine. Pure Appl Chem 79:2325–2338
Pyle AM (1993) Ribozymes: a distinct class of metalloenzymes. Science 261:709–714
Rashin AA, Honig B (1985) Reevaluation of the born model of ion hydration. J Phys Chem 89:5588–5593
Reinhard CT, Planavsky NJ, Gill BC, Ozaki K, Robbins LJ, Lyons TW, Fischer WW, Wang C, Cole DB, Konhauser KO (2017) Evolution of the global phosphorus cycle. Nature 541:386–389
Rittié L, Perbal B (2008) Enzymes used in molecular biology: a useful guide. J Cell Commun Signal 2:25–45
Robertson MP, Scott WG (2007) The structural basis of ribozyme-catalyzed RNA assembly. Science 315:1549–1553
Scott WG (2007) Ribozymes. Curr Opin Struct Biol 17:280–286
Shcherbakova I, Mitra S (2009) Hydroxyl-radical footprinting to probe equilibrium changes in RNA tertiary structure. Methods Enzymol 468:31–46
Smith MA, Zhu X, Tabaton M, Liu G, McKeel DW Jr, Cohen ML, Wang X, Siedlak SL, Dwyer BE, Hayashi T et al (2010) Increased iron and free radical generation in preclinical alzheimer disease and mild cognitive impairment. J Alzheimers Dis 19:363–372
Steitz TA (1999) DNA polymerases: structural diversity and common mechanisms. J Biol Chem 274:17395–17398
Theil EC, Goss DJ (2009) Living with iron (and oxygen): questions and answers about iron homeostasis. Chem Rev 109:4568–4579
Torrents E, Aloy P, Gibert I, Rodriguez-Trelles F (2002) Ribonucleotide reductases: divergent evolution of an ancient enzyme. J Mol Evol 55:138–152
Tullius TD, Dombroski BA (1985) Iron (II) EDTA used to measure the helical twist along any DNA molecule. Science 230:679–681
Tullius TD, Greenbaum JA (2005) Mapping nucleic acid structure by hydroxyl radical cleavage. Curr Opin Chem Biol 9:127–134
Ushizaka S, Kuma K, Suzuki K (2011) Effects of Mn and Fe on growth of a coastal marine diatom *Talassiosira weissflogii* in the presence of precipitated Fe(III) hydroxide and EDTA-Fe(III) complex. Fish Sci 77:411–424
Uudsemaa M, Tamm T (2004) Calculation of hydration enthalpies of aqueous transition metal cations using two coordination shells and central ion substitution. Chem Phys Lett 400:54–58
Vary CP, Vournakis JN (1984) RNA structure analysis using methidiumpropyl-EDTA.Fe(II): a base-pair-specific RNA structure probe. Proc Natl Acad Sci USA 81:6978–6982
Vicens Q, Gooding AR, Laederach A, Cech TR (2007) Local RNA structural changes induced by crystallization are revealed by shape. RNA 13:536–548
Wilkinson KA, Merino EJ, Weeks KM (2005) RNA shape chemistry reveals nonhierarchical interactions dominate equilibrium structural transitions in tRNA(Asp) transcripts. J Am Chem Soc 127:4659–4667
Wilkinson KA, Gorelick RJ, Vasa SM, Guex N, Rein A, Mathews DH, Giddings MC, Weeks KM (2008) High-throughput shape analysis reveals structures in Hiv-1 genomic RNA strongly conserved across distinct biological states. PLoS Biol 6:883–899

Wolfe-Simon F, Starovoytov V, Reinfelder JR, Schofield O, Falkowski PG (2006) Localization and role of manganese superoxide dismutase in a marine diatom. Plant Physiol 142:1701–1709

Wulfsberg G (1991) Principles of descriptive inorganic chemistry. University Science Books, Sausalito, CA

Yang W, Lee JY, Nowotny M (2006) Making and breaking nucleic acids: two-Mg^{2+}-ion catalysis and substrate specificity. Mol Cell 22:5–13

Yin YW, Steitz TA (2004) The structural mechanism of translocation and helicase activity in T7 RNA polymerase. Cell 116:393–404

Zheng H, Shabalin IG, Handing KB, Bujnicki JM, Minor W (2015) Magnesium-binding architectures in RNA crystal structures: validation, binding preferences, classification and motif detection. Nucleic Acid Res 43:3789–3801